Vol. 9, No. 1, pp. 12-20, June 2010

INTERNATIONAL JOURNAL OF SAFETY
www.kosos.or.kr

Fatigue Assessment of Steel Railway Bridge by Service Loading about 65 Years

Sung-Wook Hong*, Won-Kyu Chai[1] and Myeong-Gu Lee[2]

Dept. of Civil Engineering, Hallym College, ChoonCheon, GangWon 200-711, Korea
[1]Dept. of Construction Information, Shingu University, SeongNam, GyeongGi 462-743, Korea
[2]Health and Safety Engineering Major, EulJi University, SeongNam, GyeongGi 461-713, Korea

(Received March 25, 2010, Accepted June 10, 2010)

Abstract : In this study, a series of random field test and dynamic analysis in the time domain were carried out in order to find in the reason of fatigue damage of the main and the secondary members in the 3-span continuous steel plate girder railway bridge being under in service over 60 years. From the measured and the analyzed results, the stress distribution patterns were investigated for the members with fatigue damage. In addition, global and local numerical stress analysis was performed for the members damaged severely by corrosion, to estimate variation of the distribution by corrosion. Finally, a reasonable cut-off ratio in the steel plate railway bridge will be proposed by analyzing the equivalent stress ranges according the ratio.

Key words: fatigue analysis, fatigue damage, steel plate girder railway bridge, cut-off ratio, equivalent stress range

1. Introduction

There are about 2,500 railway bridges in Korea. The length of steel bridges occupies about 48% of the total length, and the component ratio according to the bridge types is shown in Fig. 1(a). Also, from the distribution characteristics according to the serviced year in steel bridges as shown in Fig. 1(b), the number of steel bridges being under in service more than 50 years is about 46%.

The fatigue and corrosion damages are the major factors affecting the life of steel bridges in the deteriorated steel bridges, and these damages are accumulated as time goes by. In addition, a number of examples of damages are being frequently reported on the focus of the non-ballastic steel railway bridges whose dead loads are small, and the variations of live load stresses are large. For the above reasons, a number of case studies on repair and retrofits are conducted vigorously in Korea.

In this study, a series of field test and finite element analysis have been performed in order to assess the

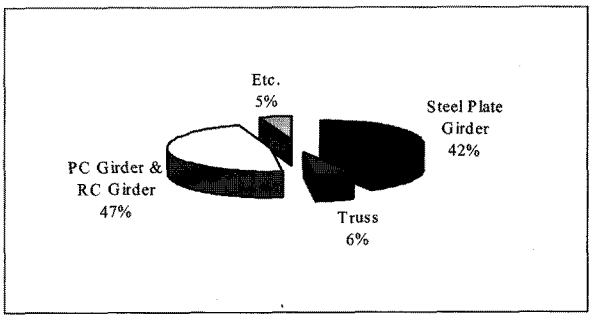

(a) **Classification according to bridge length**

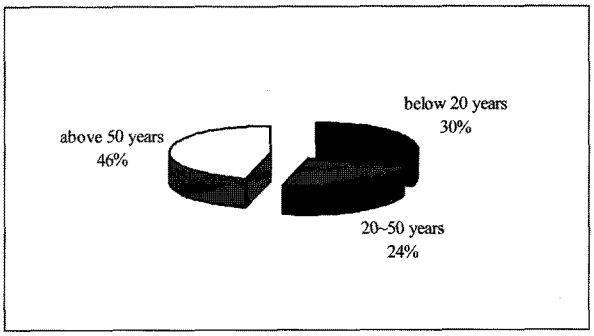

***(b)* Classification according to serviced year**

Fig. 1. Situations of railway bridges in Korea.

*Corresponding author: swhong@hsc.ac.kr

Table 1. Synopsis of object bridge

Bridge Name	Railway Bridge
Year for the completion	1944. 6.
Superstructure	3-span continuous SPG bridge 3-span continuous steel truss bridge (truss type : complex truss) simple span steel truss bridge (truss type : warren truss)

stress characteristics according to the degree of deterioration of the non-ballastic steel plate girder railway bridge being under in service about 60 years.

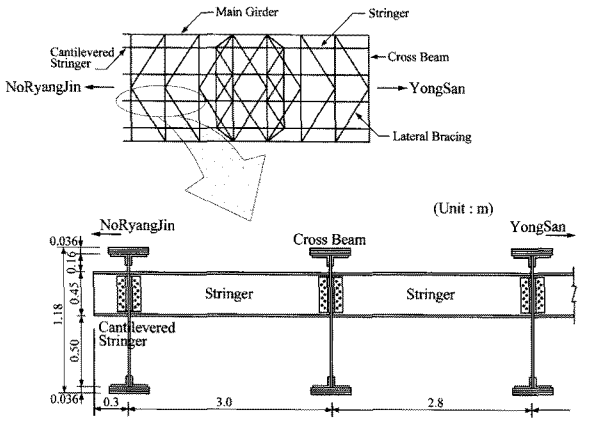

(*a*) side view

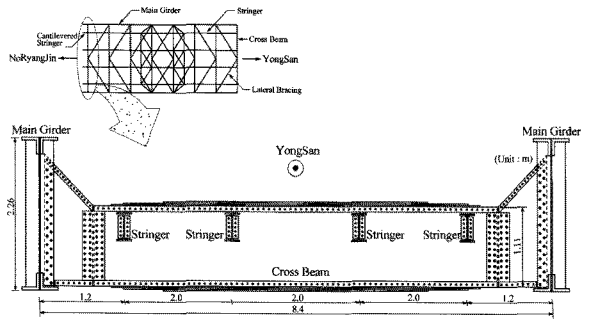

(*b*) cross-sectional view

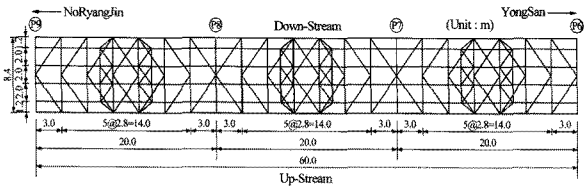

(*c*) plan view

Fig. 2. Synopsis of object bridge.

2. Synopsis of object Bridge

The superstructure of the object bridge in this study consists of 3-span continuous steel plate girder bridges(total length is 482 m), and 3-span continuous and simple span steel truss bridges(total length is 630 m) as shown in Table 1 and Fig. 2. This bridge is being under in service about 60 years as mentioned above.

The 3-span continuous steel plate girder bridge has

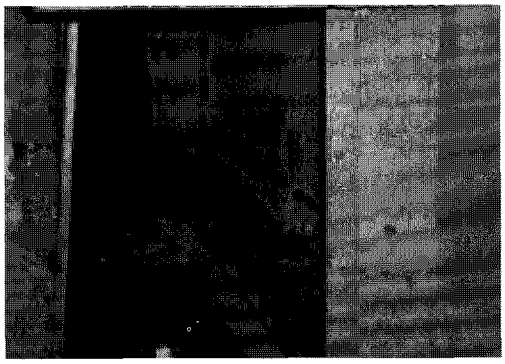

(*a*) Corrosion in cross beam

(*b*) Fatigue crack in the connection

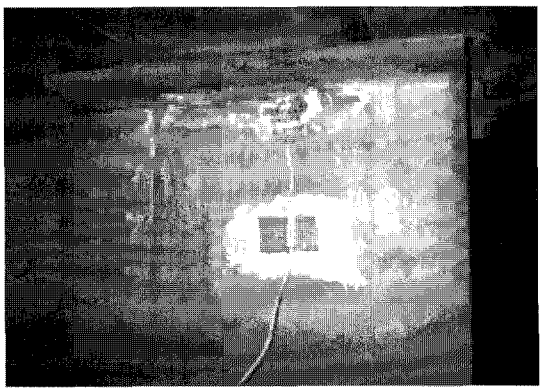

(*c*) Fatigue crack in cantileverd stringer between main girder & cross beam

Fig. 3. Deteriorations of steel plate girder section.

been selected for this study which has corrosion damages and fatigue cracks as shown in Fig. 3.

3. Attachment of Strain Gauge

Uni-axial strain gauges have been used in order to measure the nominal stresses at lower flange of main girder (gauge no. : 1), lower flange of stringer (gauge no. : 3) of center part, and upper flange of main girder(gauge no. : 2), lower flange of cross beam (gauge no. : 4) above pier P9 as shown in Fig. 4.

Also, as shown in Fig. 5 and Fig. 6, uni-axial strain gauges have been used in order to measure the local stresses at crack tips in the perpendicular direction of fatigue crack at the connection between main girder and cross beam (gauge no. : 9, 10) and cantilevered stringer (gauge no. : 5, 6) which has fatigue crack as shown in Fig. 3(*b*), (*c*). And strain rossettes have been used in order to measure the principal stresses at the connection between main girder and cross beam (gauge no. : 11, 12) and cantilevered stringer (gauge no. : 7, 8) which has not fatigue crack. The gauge number in parenthesis in Fig. 5 and Fig. 6 means the strain gauge which has been attached in the opposite face of the same members in order to measure the out-of-plane stress

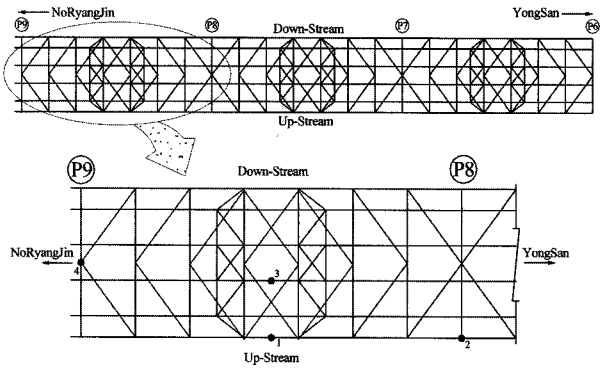

Fig. 4. Gauge attachment points in main members.

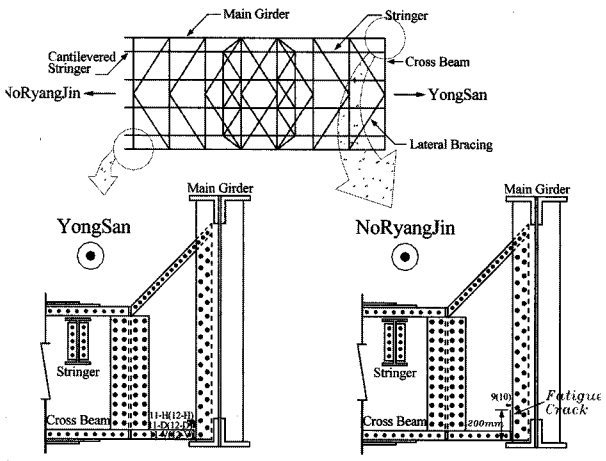

Fig. 5. Gauge attachment points in the connection between main girder & cross beam.

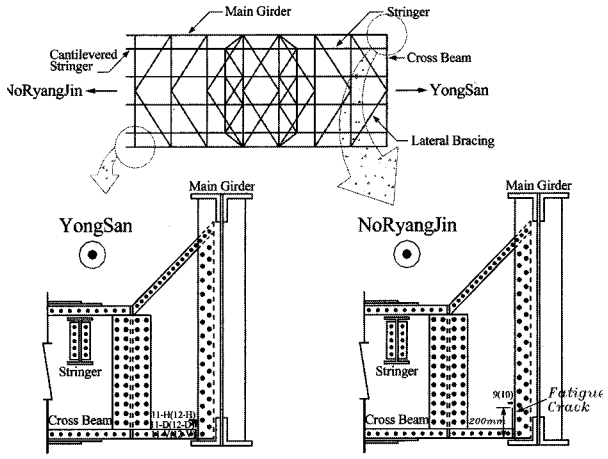

Fig. 6. Gauge attachment points in cantilevered stringer.

4. Field Test Results

Typical stress histories at each main members from the field test are shown in Fig. 7. The stress range of stringer is larger than that of main girder and cross beam, and the effect of bogie loads is remarkable as shown in Fig. 7. Examples of stress histories at crack tip which have been measured at the cracked position of web of cross beam (gauge no. : 9, 10) in the connection between main girder and cross beam are shown in Fig. 8.

From Fig. 8, it is known that stress levels at this crack tip are relatively low and compressive component is dominant due to inappropriate gauge attachment. Therefore, further analysis of the measured stresses at this point is not performed. Also, examples of principal stress histories which have been measured in the uncracked position of web of cross beam (gauge no. : 11, 12) in the connection between main girder and cross beam are shown in Fig. 9.

From Fig. 9, it is known that the large compressive components of stresses are occurred due to the connection type which the web of cross beam is partially restrained by the main girder. As seen from Fig. 9, because the measured principal stress histories are quite different at inside and outside faces, the in-plane and the out-of-plane stress histories are calculated from Fig. 9 and shown in Fig. 10.

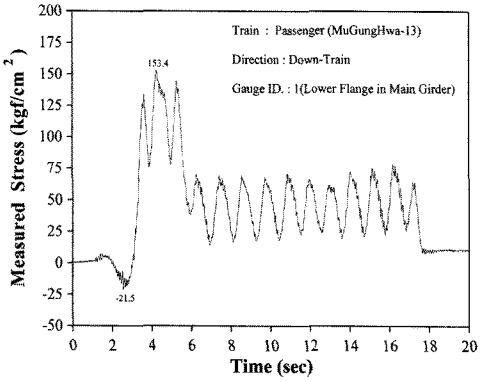

(*a*) Lower flange of main girder

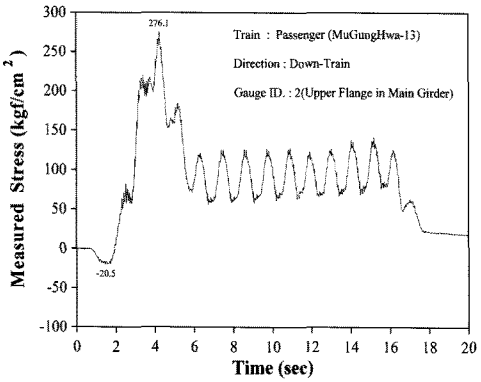

(*b*) Upper flange of main girder

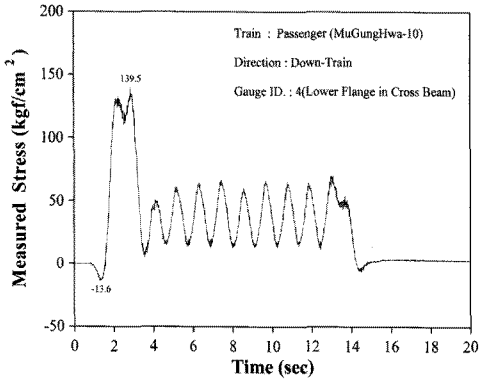

(*c*) Lower flange of cross beam

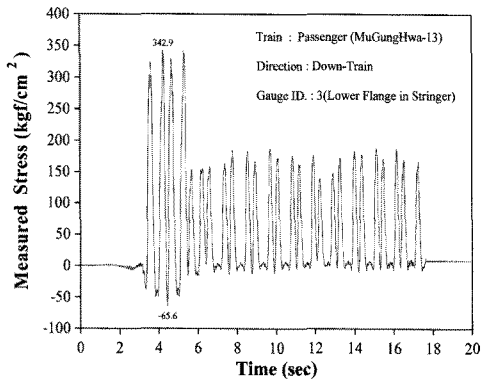

(*d*) Lower flange of stringer

Fig. 7. Examples of stress histories in main members.

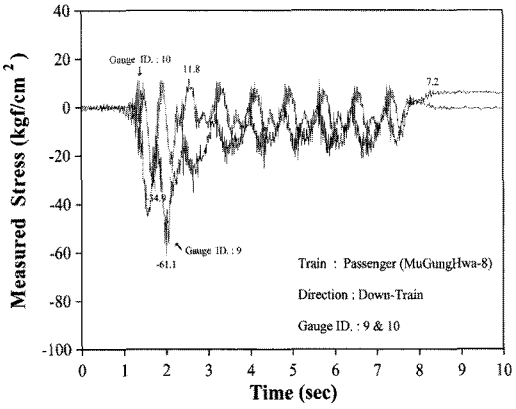

(*a*) In case of down-train

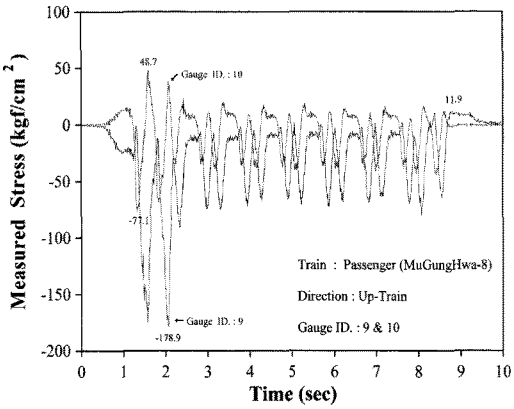

(*b*) In case of up-train

Fig. 8. Examples of stress histories.

From Fig. 10, it is known that the out-of-plane stress exceeds the in-plane stress. From these results, it can be said that the out-of-plane deformation is the main reason of the fatigue crack at this connection.

Meanwhile, examples of stress histories which are acquired by the strain gauges being attached in the vertical direction at up-stream face (gauge no. : 5) and down-stream face (gauge no. : 6) of the cracked cantilevered stringer of Fig. 6 are shown in Fig. 11.

As shown in Fig. 11, compressive stress is mainly occurred in the gauge attached on the down-stream face, and tensile stress on up-stream. Fig. 12 shows the in-plane and the out-of-plane stress histories which are obtained from the result of Fig. 11.

As shown in Fig. 12, the out-of-plane stress is more dominant than the in-plane stress in the cracked cantilevered stringer.

In addition, examples of principal stress histories which are acquired by the strain gauges being attached at up-stream face (gauge no. : 7) and down-stream face (gauge no. : 8) of the uncracked cantilevered stringer

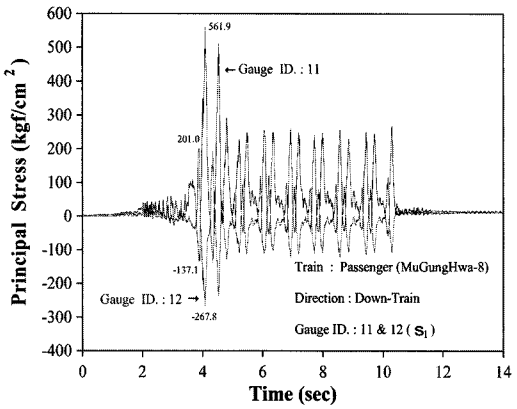

(*a*) In case of down-train

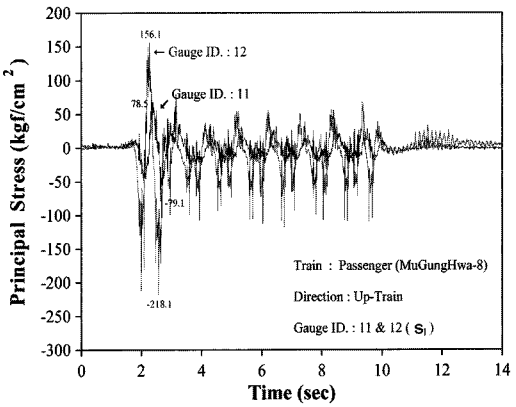

(*b*) In case of up-train

Fig. 9. Examples of principal stress.

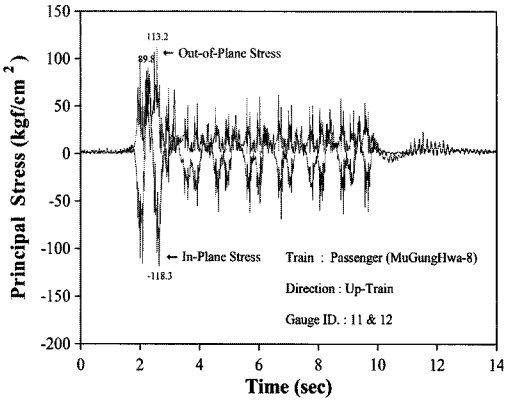

(*a*) In case of down-train

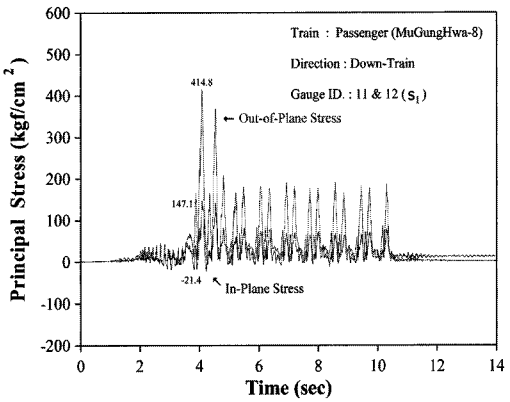

(*b*) In case of up-train

Fig. 10. Examples of in-plane & out-of-plane stress histories.

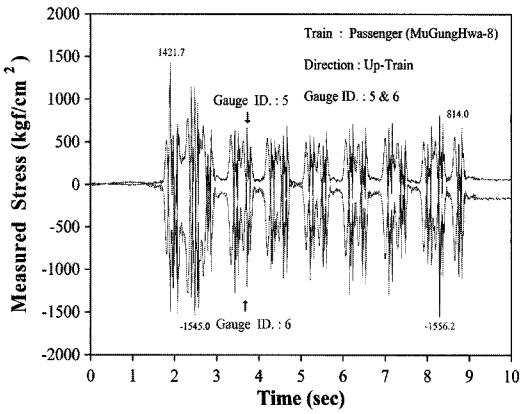

Fig. 11. Examples of stress histories in cracked cantilevered stringer.

are shown in Fig. 13. As shown in the figure, compressive stress is mainly occurred in the gauge (gauge no. : 7) attached in down-stream face, and tensile stress in up-stream.

Fig. 14 shows the in-plane and the out-of-plane stress histories obtained from Fig. 13. From Fig. 14, the out-of-plane stress is about 3 times larger than the in-plane stress at the uncracked cantilevered stringer.

The large amount of the out-of-plane stress, it is thought, is attributed by the inward deformation of the upper part of stringer when train is passing, and can be said the main reason of the crack.

Meanwhile, Fig. 15 and Fig. 16 show the results of the equivalent stresses calculated by RMC method and fatigue lives calculated by the modified Miner's rule according to the cut-off ratios in order to suggest a reasonable value of the ratio in the railway bridge. From these figures, it can be said that 15% cut-off ratio is reasonable when conducting the fatigue safety assessment of the railway bridge.

5. Finite Element Analysis

Time history analysis has been executed in order to

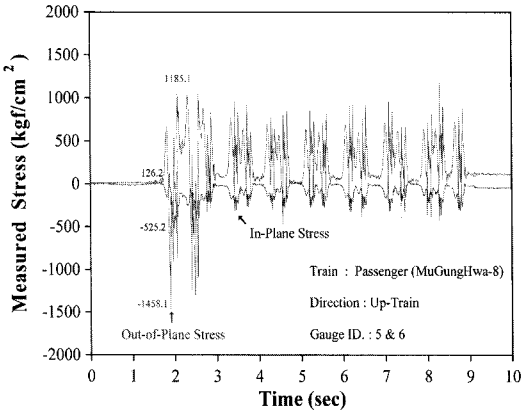

Fig. 12. Examples of in-plane & out-of-plane stress histories in cracked cantilevered stringer.

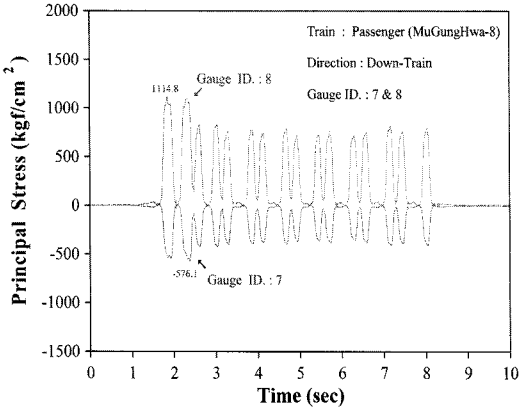

Fig. 13. Examples of principal stress histories in uncracked cantileverd stringer.

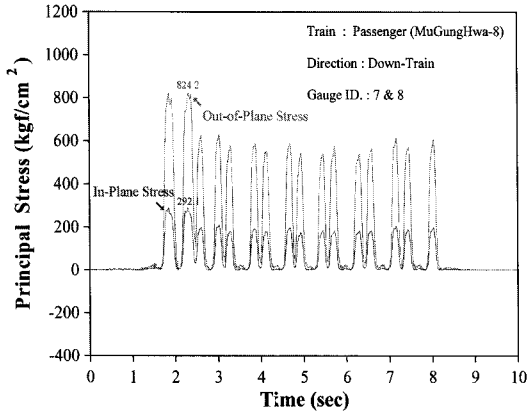

Fig. 14. Examples of in-plane & out-of-plane stress histories in uncracked cantilevered stringer.

assess the variation of the stress characteristics according to the degree of corrosion damage because the damage has been found at many parts of the bridge as

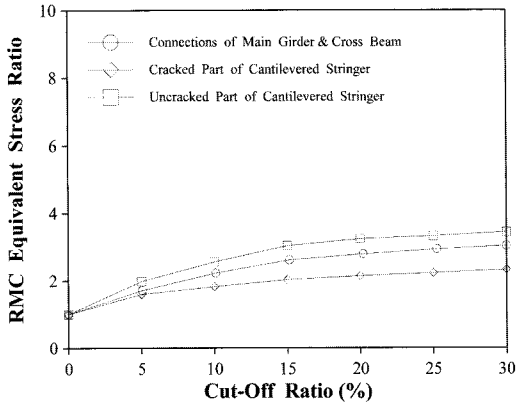

Fig. 15. Calculated equivalent stresses according to the cut-off ratio of each parts.

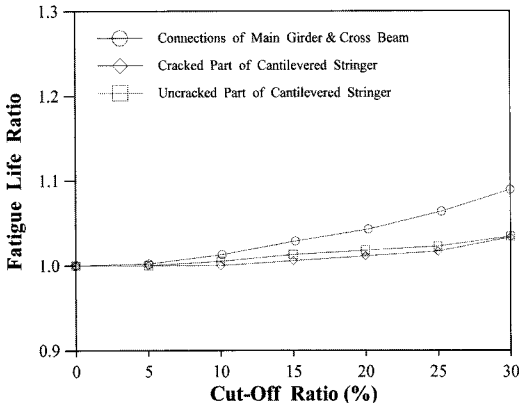

Fig. 16. Calculated fatigue lives according to the cut-off ratio of each parts.

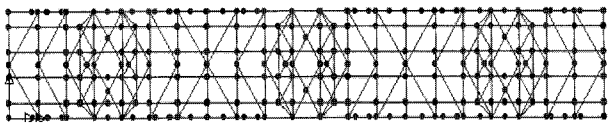

Fig. 17. Finite element analysis model of the bridge.

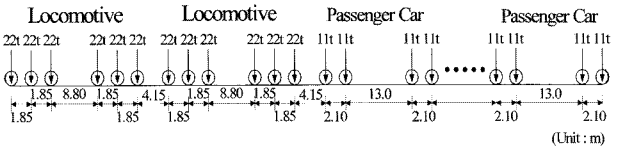

Fig. 18. Model of train load (locomotive 2 + passenger 11).

shown in Fig. 3. In this study, the amount of corrosion has been estimated assuming that the rate of corrosion follows the exponential function of Eq.(1) under the atmospheric condition of the bridge.

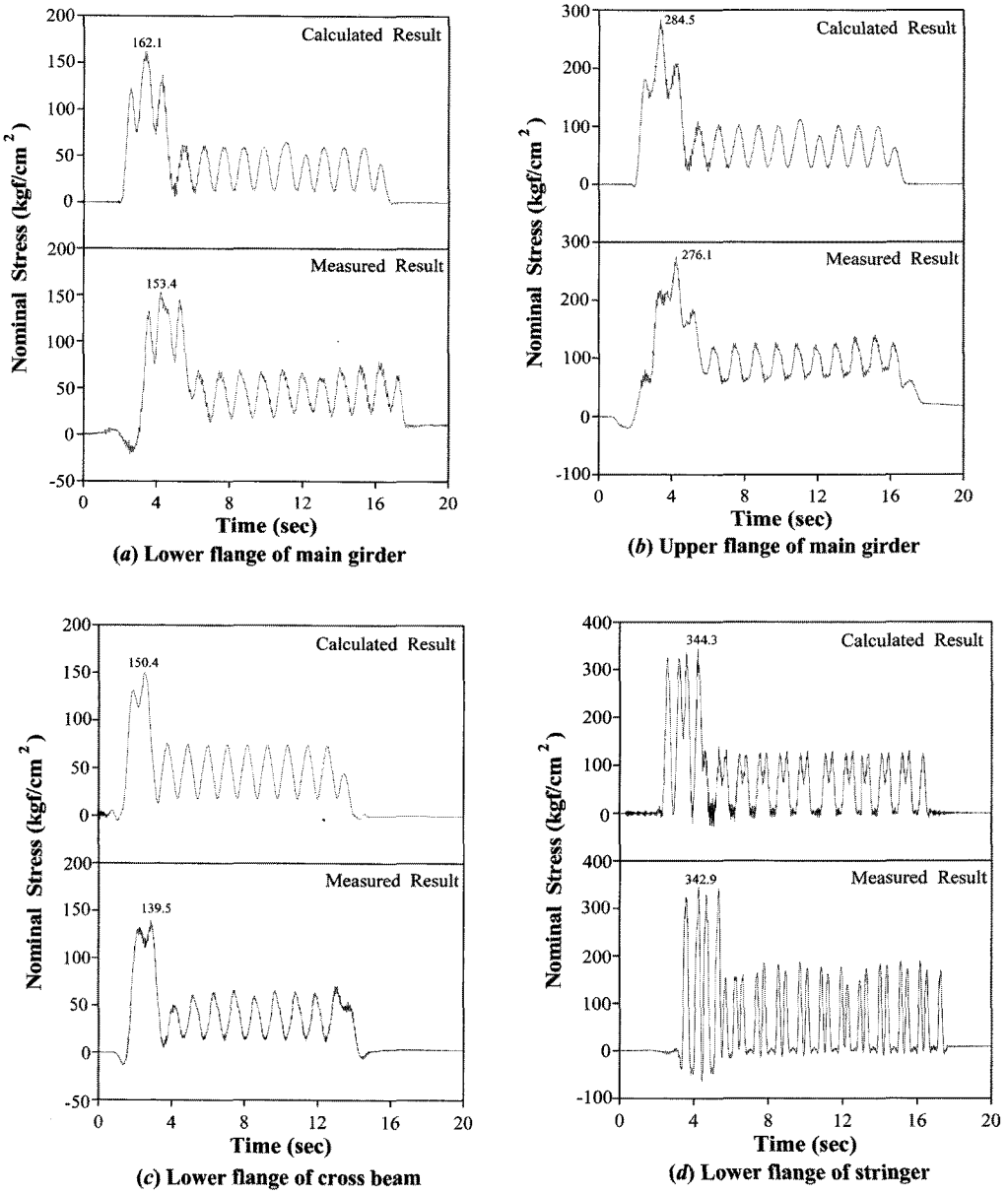

Fig. 19. Comparison of the results of time history analysis and field test in main members.

$$C = At^B \quad (1)$$

where, C means the average corrosion depth, t time in year, and A & B mean the coefficients which are acquired from the test results.

Considering the serviced year of the bridge, the corrosion depth becomes 1.8 mm when calculating the depth from Eq.(1). Therefore, in this study, the stress histories are simulated by changing the depth from 0.5 mm to 2.0 mm.

Time history analysis has been executed assuming the structure and train models as shown in Fig. 17 and Fig. 18 respectively. But, axle loads of train are considered to be constant during train passing.

6. Finite Element Analysis Result

6.1 Comparison with Field Test Results

Fig. 19 compares the stress histories of main members from the time history analysis and the field test in order to verify the validity of the analysis. From these figures, it can be said that the results coincides enough for further study.

6.2 Time History Analysis Considering Corrosion

A series of time history analysis has been executed

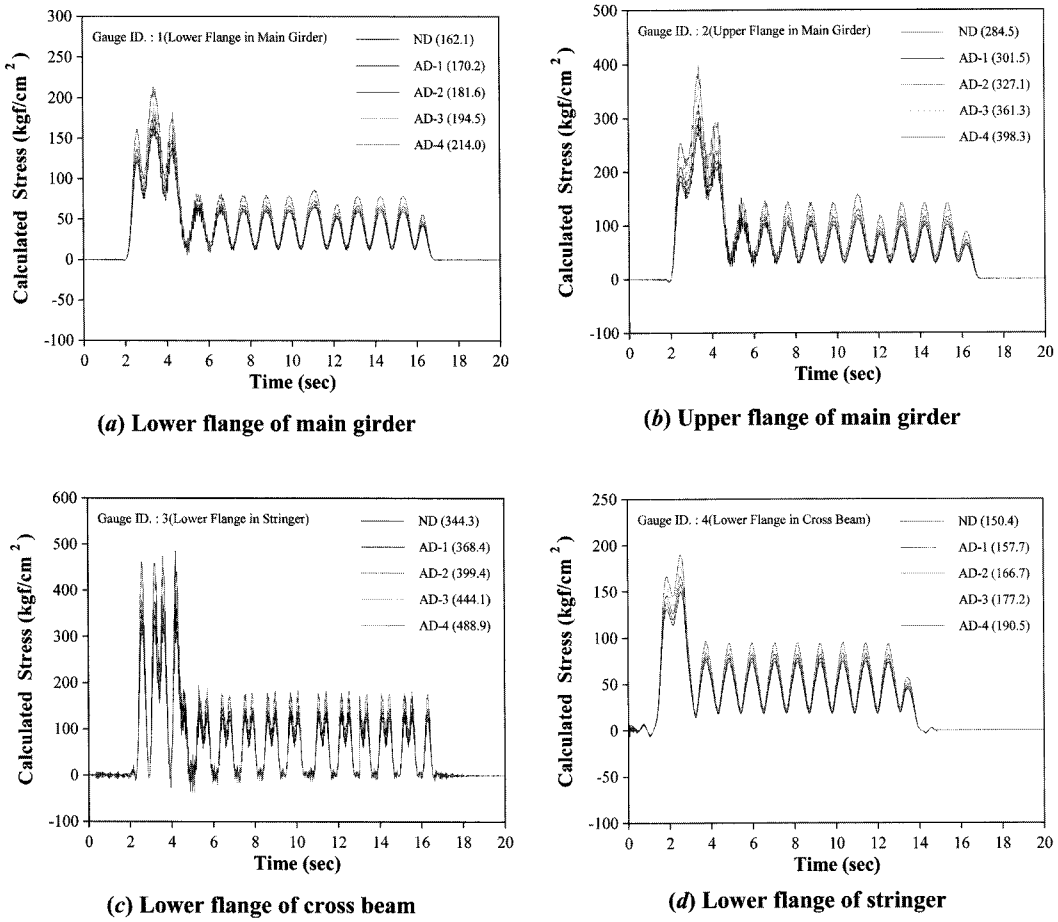

Fig. 20. Time history analysis results of main members considering corrosion.

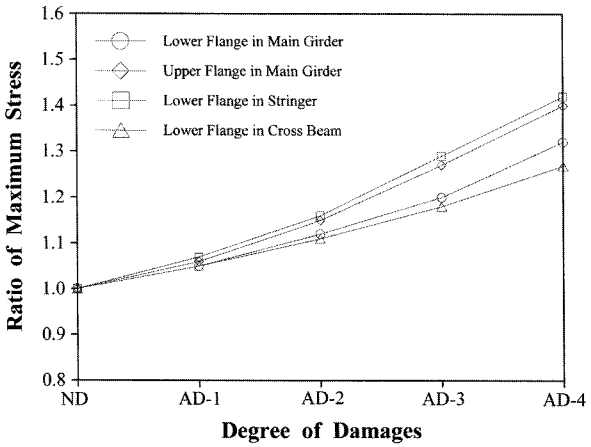

Fig. 21. Variation of maximum stresses of main members depending on degree of corrosion.

on the main members in cases of non damage(ND), damage of 0.5 mm(AD-1), damage of 1.0 mm(AD-2), damage of 1.5 mm(AD-3) and damage of 2.0 mm(AD-4). The stress histories according to the degree of damage are shown in Fig. 20.

Also, based on the result of Fig. 20, the variation of the maximum stresses of the main members are shown in Fig. 21 depending upon the degree of damage.

As shown in Fig. 20 and Fig. 21, the maximum stresses increase almost linearly according to the depth, and the increasing rate is rapid in the member with high stress.

7. Conclusions

(1) The fatigue cracks of the bridge have been caused by the effect of the out-of-plane stress.

(2) It is suggested to use 15% cut-off ratio when conducting the fatigue safety assessment of the railway bridge.

(3) From FEM analysis, it is known that the effect of section loss due to corrosion becomes large for the member with high stress occurring, therefore, the stringer is the most sensitive member for corrosion in the railway bridge.

References

[1] JSCE, "*Assessment of Deterioration and Damage in Steel Bridges*", Marugen Co. LTD., pp. 10-12, 1996.

[2] C. Miki, W. Nishigawa, J.W. Fisher, "*Inspection of Fatigue Damage in Steel Bridges*", Bridge & Foundation, pp. 17-21, 1986.

[3] P. Albrecht, A.H. Naeemi, "*Performance of Weathering Steel in Bridges*", Report No. 272, Nat. Cooperative Highway Res. Program, 1984

[4] M.E. Komp, "*Atmospheric Corrosion Ratings of Weathering Steels - Calculations and Significance*", Materials Performance, Vol. 26, No.7, pp. 42-44, 1987.

[5] B.H. Lee, "*A Study on the Stress Distribution Characteristics of Steel Truss Railway Bridges*", A Dissertation of Masters Degree, pp. 7-8, 1997.

[6] S.W. Lee, "*Maintenance of Railway Steel Structures*", Journal of KSCE, Vol. 12, No. 3, pp. 30-35, 2000.

[7] T.H. Jeong, "*An Effect on the Health of Steel Railway Bridges due to Corrosion Loss*", A Dissertation of Masters Degree, pp. 1-3, 2000.